A98-37386

AIAA-98-4547

OPTIMAL INTERCEPTION OF A MANEUVERING LONG RANGE MISSILE

Nguyen X. Vinh,* Pierre T. Kabamba† and Tetsuya Takehira‡

The University of Michigan, Ann Arbor, MI 48109-2140, U.S.A.

Abstract

In a Newtonian central force field, the minimum-fuel interception of a satellite, or a ballistic missile, in elliptic trajectory can be obtained via Lawden's theory of primer vector. To secure interception when the target performs evasive maneuvers, a new control law, with explicit solutions, is implemented. It is shown that by a rotation of coordinate system, the problem of three-dimensional interception is reduced to a planar problem. The general case of planar interception of a long range ballistic missile is then studied. Examples of interception at a specified time, head-on interception and minimum-fuel interception are presented. In each case, the requirement for the thrust acceleration is expressed explicitly as a function of time.

Introduction

The problem of minimum-fuel interception of a satellite, or a ballistic missile, in elliptic trajectory has been discussed in Ref.[12] via Lawden's theory of the primer vector. This assumes that the motion of the target is uncontrolled and is subject only to a Newtonian gravitational attraction. In that case, optimal interception is achieved by application of one or two impulses to change the trajectory of the interceptor for a collision with the target. The initial trajectory of the interceptor may be a Keplerian orbit or an atmospheric ascent trajectory of a rocket or an airplane which carries the interceptor.

In practice, the preliminary determination of the trajectory of the target is generally not perfect, and if after its release the interceptor is unguided, it will miss the target because of errors in the input data. On the other hand, the same type of failed interception will occur if the target performs evasive maneuvers during the last portion of its course. To secure interception, it is proposed in this paper to use an improved guidance law, first discussed by Cochran in Ref.[2], and later generalized and solved in closed form by the present authors in Ref.[11].

The general consideration for interception, the condition for interception at a specified point, and the condition for head-on interception are derived. For a fixed time interception, after solving the Lambert problem to obtain the reference trajectory, the guidance law is implemented with two navigation constants. In the case of a maneuvering target, the thrust vector, in magnitude and direction, for the guidance of the interceptor is presented explicitly as a function of time and it is clearly shown that the thrust level remains small for small deviation of the target.

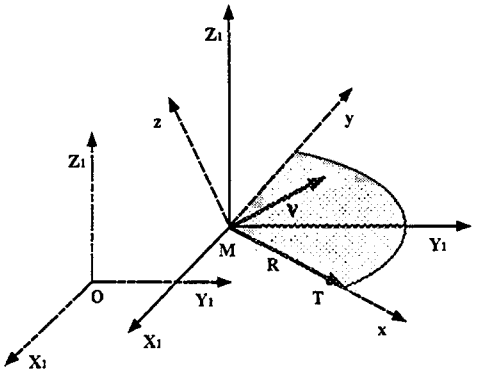

Fig. 1: Coordinate Systems.

Guidance Law

The basic coordinate systems are presented in Fig. 1 with $OX_1Y_1Z_1$ being an inertial system and

*Professor, Department of Aerospace Engineering, Senior Member AIAA.

†Professor, Department of Aerospace Engineering.

‡Doctoral Candidate, Department of Aerospace Engineering, Student Member AIAA.

$Mxyz$ being the moving coordinate system with origin at the position of interceptor M, the x-axis being along the line-of-sight from M to the target position T, and the Mxy plane being the plane of relative motion which contains the relative position vector $\mathbf{R}$ and the relative velocity vector $\mathbf{V}$. The z-axis is orthogonal to both $\mathbf{R}$ and $\mathbf{V}$, but has the positive direction parallel to $\mathbf{R}_0 \times \mathbf{V}_0$. Then the y-axis completes the right hand coordinate system with $\hat{\mathbf{i}}$, $\hat{\mathbf{j}}$ and $\hat{\mathbf{k}}$ being the unit vectors along the axes.

Let $\mathbf{R}_M$ and $\mathbf{R}_T$ be respectively, the position vector of the interceptor and the target. The relative position vector and relative velocity vector are

$$\mathbf{R} = \mathbf{R}_T - \mathbf{R}_M = R\,\hat{\mathbf{i}}, \tag{1}$$

and

$$\mathbf{V} = \dot{\mathbf{R}} = \dot{R}\,\hat{\mathbf{i}} + R\,\omega \times \hat{\mathbf{i}}, \tag{2}$$

where ω is the angular velocity vector of the rotating frame $Mxyz$. In inertial space, the orientation of this rotating frame is specified by the Euler angles δ, ϕ and β as shown in Fig. 2. They are related to the components of ω in the rotating axes as follows:

$$\omega_x = \dot{\delta}\sin\phi\sin\beta + \dot{\phi}\cos\beta, \tag{3a}$$

$$\omega_y = \dot{\delta}\sin\phi\cos\beta - \dot{\phi}\sin\beta, \tag{3b}$$

$$\omega_z = \dot{\beta} + \dot{\delta}\cos\phi. \tag{3c}$$

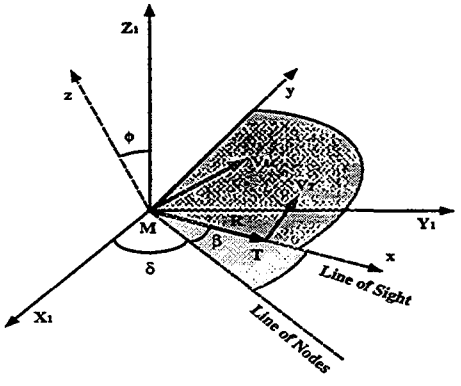

Fig. 2: Euler Angles.

As a guidance law, we define the generalized commanded relative acceleration

$$\mathbf{A}_c = k_2 \dot{R}\,\omega_z\,\hat{\mathbf{i}} + k_1 \dot{R}\,\omega_z\,\hat{\mathbf{j}}, \tag{4}$$

where k_1 and k_2 are navigation constants. In Cochran's analysis [2], $k_2 = 0$ while the navigation constant k_1 takes on the values 3 and 4 for the integrable cases. Here, however, both parameters k_1 and k_2 are real and arbitrary.

The objective of the guidance is to select navigation constants k_1, k_2 and initial conditions in order to drive R to zero within the performance capabilities of the interceptor.

It has been shown that, as a result of this law, both the precession angle δ and nutation angle ϕ are constant and consequently the Mxy plane remains parallel to the initial plane of relative motion Ref.[11]. Therefore, even for the case of three-dimensional interception, the solution is obtained by solving for the range $R(t)$ and the rotation angle $\beta(t)$ as function of the time t in the translating Mxy plane. With M_0 as the origin of coordinates, we take the inertial OXY plane to be the initial plane of relative motion defined by $\mathbf{R}_0$ and $\mathbf{V}_0$. While both points M and T move in the inertial space, the line-of-sight MT generates a ruled surface as shown in Fig. 3. We compute the coordinates of the interceptor by the relations

$$X_M = X_T - R\cos\beta, \tag{5a}$$

$$Y_M = Y_T - R\sin\beta, \tag{5b}$$

$$Z_M = Z_T, \tag{5c}$$

which are valid for arbitrary motion of the target X_T, Y_T and Z_T.

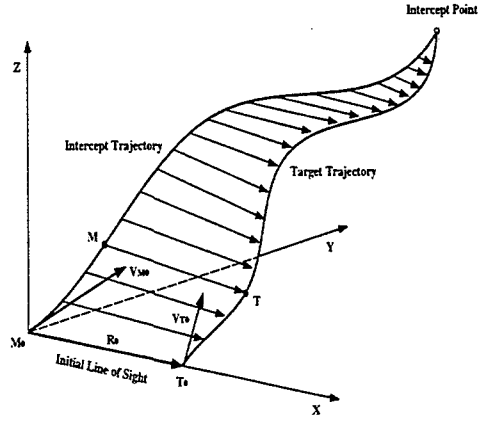

Fig. 3: Ruled Surface and Generators.

By using the initial distance R_0 as unit distance, we define the normalized relative distance

$$r = \frac{R}{R_0}. \tag{6}$$

In the plane of relative motion, it has been shown that if the guidance law (4) is implemented, and with a dimensionless time defined as

$$\tilde{\tau} = \omega_{z0} t, \tag{7}$$

where $\omega_{z0} = (d\beta/dt)_0$ is the initial rate of rotation

of the line-of-sight, the variations of r and β are governed by the third order nonlinear system [11]

$$r'' = k_2 r^{k_1-2} r' + r^{2k_1-3}, \quad (8a)$$

$$\beta' = r^{k_1-2}, \quad (8b)$$

subject to the initial condition

$$r(0) = 1, \; r'(0) = u_0, \; \beta(0) = \beta_0. \quad (9)$$

We have obtained explicit solutions for this nonlinear system in the form

$$r^{k_1-1} = \frac{k_1-1}{K}\left\{(u_1-u_0)\exp\left[\frac{m-1}{2}K(\beta-\beta_0)\right] - (u_2-u_0)\exp\left[\frac{m+1}{2}K(\beta-\beta_0)\right]\right\}, \quad (10)$$

where by definition

$$K = \sqrt{k_2^2 + 4(k_1-1)} > |k_2|, \quad (11a)$$

$$-1 < m = \frac{k_2}{K} < 1, \quad (11b)$$

$$u_1 = \frac{k_2+K}{2(k_1-1)} > 0, \quad (11c)$$

$$u_2 = \frac{k_2-K}{2(k_1-1)} < 0. \quad (11d)$$

To achieve interception, the value u_0 of the initial closing speed selected must satisfy the condition

$$u_0 < u_2. \quad (12)$$

The solution for the dimensionless time as function of the line-of-sight swept angle is given by

$$\tilde{\tau} = \frac{1}{K a^p}\left[\frac{K}{(k_1-1)(u_1-u_0)}\right]^{(1-q)} [B_x(p,q) - B_a(p,q)] + \tilde{\tau}_0, \quad (13)$$

where $B_x(p,q)$ is the incomplete beta function [1]

$$B_x(p,q) = \int_0^x s^{(p-1)}(1-s)^{q-1} ds, \quad (14)$$

where s is a dummy variable and the argument x is defined as

$$x = a \exp[K(\beta-\beta_0)], \quad (15)$$

and it varies between a and 1. The parameters p, q and a depend on the guidance constants k_1 and k_2 through the relations

$$0 \le a = \frac{u_2-u_0}{u_1-u_0} < 1, \quad (16a)$$

$$0 < q = \frac{1}{k_1-1} \le 1, \quad (16b)$$

$$0 \le p = \frac{1}{2}(1-m)(1-q) < 1. \quad (16c)$$

Using these analytical solutions, the final value of the line-of-sight angle can be easily calculated by setting $r = 0$ in Eq.(10) to obtain

$$\beta_f = \frac{1}{K}\log\left(\frac{u_1-u_0}{u_2-u_0}\right) + \beta_0. \quad (17)$$

Moreover, since $x_f = 1$ in Eq.(15), substituting $x = x_f$ into Eq.(13), we have the intercept time as the final value of $\tilde{\tau}$

$$\tilde{\tau}_f = \frac{1}{K a^p}\left[\frac{K}{(k_1-1)(u_1-u_0)}\right]^{(1-q)} [B(p,q) - B_a(p,q)] + \tilde{\tau}_0, \quad (18)$$

where $B(p,q)$ is the beta function defined as [1]

$$B(p,q) = \int_0^1 s^{(p-1)}(1-s)^{q-1} ds. \quad (19)$$

Application to 3-D Interception

After we project the target motion into the initial plane of relative motion M_0XY, we can separate the X- and Y-directional target motion from the Z-directional one in the inertial coordinate system M_0XYZ. Since the relative motion is independent of the target motion, we can consider the guidance problem in the M_0XY plane using Eqs.(5). As an example, we now consider a case of three-dimensional interception of a target in helical motion.

In general, in the original inertial system $M_0X_1Y_1Z_1$, the motion of the target, defined by

$$\mathbf{R}_T = \mathbf{R}_T(t), \quad (20)$$

and the initial velocity $\mathbf{V}_{M0}$ of the interceptor are given. Therefore, we also have $\mathbf{R}_0 = \mathbf{R}_T(t_0)$ and $\mathbf{V}_{T0} = \dot{\mathbf{R}}_T(t_0)$. By taking R_0 as the unit distance and V_{T0} as the unit speed, we are led to a new dimensionless time τ defined as

$$\tau = \frac{V_{T0}}{R_0} t. \quad (21)$$

With lower case for dimensionless coordinates and velocity components, we consider in the original system

$$\mathbf{r}_0 = (x_{1T0}, \; y_{1T0}, \; z_{1T0}), \quad (22a)$$

$$\mathbf{v}_{T0} = (u_{1T0}, \; v_{1T0}, \; w_{1T0}), \quad (22b)$$

$$\mathbf{v}_{M0} = (u_{1M0}, \; v_{1M0}, \; w_{1M0}). \quad (22c)$$

In Fig. 2, the initial relative angular momentum $\mathbf{h} = \mathbf{r}_0 \times (\mathbf{v}_{T0} - \mathbf{v}_{M0})$ which is along the z-direction, has

components

$$h_x = y_{1T0}(w_{1T0} - w_{1M0}) - z_{1T0}(v_{1T0} - v_{1M0}), \quad (23a)$$

$$h_y = z_{1T0}(u_{1T0} - u_{1M0}) - x_{1T0}(w_{1T0} - w_{1M0}), \quad (23b)$$

$$h_z = x_{1T0}(v_{1T0} - v_{1M0}) - y_{1T0}(u_{1T0} - u_{1M0}). \quad (23c)$$

With these, we compute the Euler angles by the relations

$$\cos\phi = \frac{h_z}{\sqrt{h_x^2 + h_y^2 + h_z^2}}, \quad (24a)$$

$$\sin\phi\cos\delta = -\frac{h_y}{\sqrt{h_x^2 + h_y^2 + h_z^2}}, \quad (24b)$$

$$\sin\phi\sin\delta = \frac{h_x}{\sqrt{h_x^2 + h_y^2 + h_z^2}}, \quad (24c)$$

$$\cos\beta_0 = \cos\delta\ x_{1T0} + \sin\delta\ y_{1T0}. \quad (24d)$$

After performing a rotation of coordinate system from $M_0x_1y_1z_1$ to M_0xyz and solving for r and β, we have the coordinates of the interceptor from Eqs.(5) rewritten as

$$x_M = x_T - r\cos\beta, \quad (25a)$$

$$y_M = y_T - r\sin\beta, \quad (25b)$$

$$z_M = z_T. \quad (25c)$$

In this numerical example, we consider

$$\mathbf{r}_0 = (0.7625,\ 0.4575,\ 0.4575), \quad (26a)$$

$$\mathbf{v}_{T0} = (0.9165,\ 0,\ -0.4), \quad (26b)$$

$$\mathbf{v}_{M0} = (1.7,\ -0.85,\ 0.85), \quad (26c)$$

where $|\mathbf{r}_0| = 1$, $|\mathbf{v}_{T0}| = 1$ and $|\mathbf{v}_{M0}| = 2.0821$. Using the variable τ, we have the dimensionless equations of helical motion in the original coordinate system $M_0x_1y_1z_1$

$$x_{1T}(\tau) = x_{1T0} + a\sin(c\tau), \quad (27a)$$

$$y_{1T}(\tau) = y_{1T0} - a[1 - \cos(c\tau)], \quad (27b)$$

$$z_{1T}(\tau) = z_{1T0} + b\tau, \quad (27c)$$

and take $a = 0.7050$ for the turning radius, and $b = -0.4$ for the descent rate. This gives the horizontal speed $u_{1T0} = 0.9165$ from Eq.(26b), and since in circular motion we have $ac = u_{1T0}$, we obtain the value $c = 1.3$ for the turning rate. Now using the three initial vectors $\mathbf{r}_0$, $\mathbf{v}_{T0}$ and $\mathbf{v}_{M0}$ from Eqs.(26a), (26b) and (26c), we calculate the Euler angles as $\delta = 238.2438°$, $\phi = 48.3037°$ and $\beta_0 = 142.2146°$ for the rotation of coordinate system. In the new system M_0xyz, we have the components of the initial vectors

$$\mathbf{r}_0 = (1,\ 0,\ 0), \quad (28a)$$

$$\mathbf{v}_{T0} = (0.5158,\ 0.1219,\ -0.8480), \quad (28b)$$

$$\mathbf{v}_{M0} = (1.2962,\ -1.3913,\ -0.8480), \quad (28c)$$

where $|\mathbf{v}_{T0}| = 1$ and $|\mathbf{v}_{M0}| = 2.0821$. The transformation gives the coordinates $x_T(\tau)$, $y_T(\tau)$ and $z_T(\tau)$, while r and β are calculated by the explicit formulas in the previous section using $k_1 = 3$ and $k_2 = 1$. In applying the formulas, we take $\beta_0 = 0$, $t_0 = 0$, while the evaluation of the conversion factor A of the time scale from τ to $\bar{\tau}$ and the initial closing speed u_0 is processed as follows. In the M_0xy plane, the projections of the velocities of the target and the interceptor are represented by $\bar{\mathbf{V}}_T$ and $\bar{\mathbf{V}}_M$ directed at the heading angles θ_T and θ, respectively as shown in Fig. 4. We first have the time conversion factor

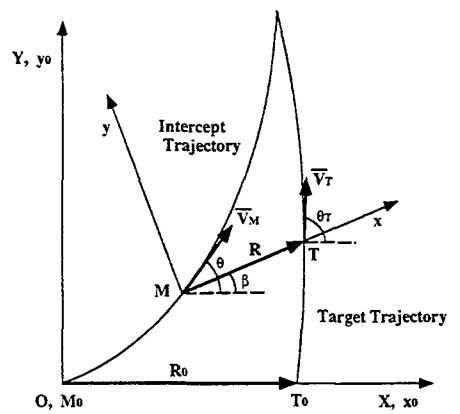

Fig. 4: Velocity Diagram in the Plane of Relative Motion.

$$A = \frac{\bar{\tau}}{\tau} = \frac{\omega_{z0}\,R_0}{V_{T0}} = \frac{\bar{V}_{T0}\sin(\theta_{T0} - \beta_0) - \bar{V}_{M0}\sin(\theta_0 - \beta_0)}{V_{T0}}. \quad (29)$$

Consequently, since $\beta_0 = 0$

$$A = v_{T0} - v_{M0}. \quad (30)$$

For the initial closing speed, we have

$$u_0 = \left(\frac{dr}{d\bar{\tau}}\right)_0 = \frac{1}{\omega_{z0}R_0}\left(\frac{dR}{dt}\right)_0 = \frac{\bar{V}_{T0}\cos(\theta_{T0} - \beta_0) - \bar{V}_{M0}\cos(\theta_0 - \beta_0)}{\bar{V}_{T0}\sin(\theta_{T0} - \beta_0) - \bar{V}_{M0}\sin(\theta_0 - \beta_0)}, \quad (31)$$

or

$$u_0 = \frac{u_{T0} - u_{M0}}{v_{T0} - v_{M0}}. \qquad (32)$$

Once we solve the guidance problem in the system M_0XYZ, we re-transform the coordinates from M_0XYZ to the original coordinate frame $M_0X_1Y_1Z_1$ to obtain the motion of the interceptor in this system.

Figure 5 shows the two trajectories in the rotated coordinate system with the line-of-sight constantly parallel to the M_0xy plane. The target trajectory and the intercept trajectory in the original system $M_0X_1Y_1Z_1$ are shown in Fig. 6.

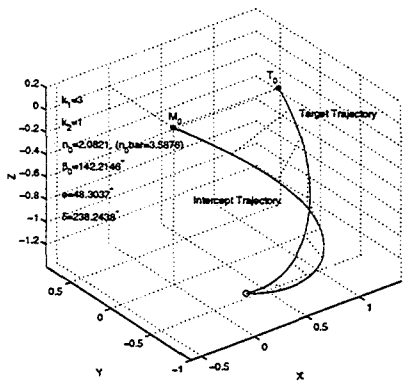

Fig. 5: 3-D Interception in M_0XYZ.

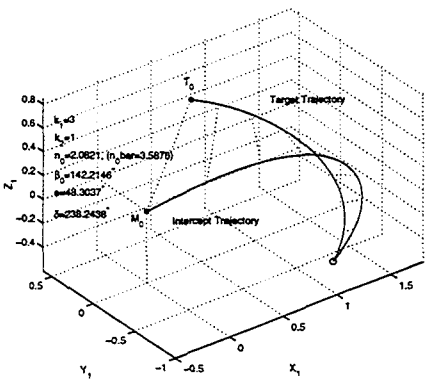

Fig. 6: 3-D Interception in $M_0X_1Y_1Z_1$.

Interception of a Long Range Ballistic Missile

General Formulation

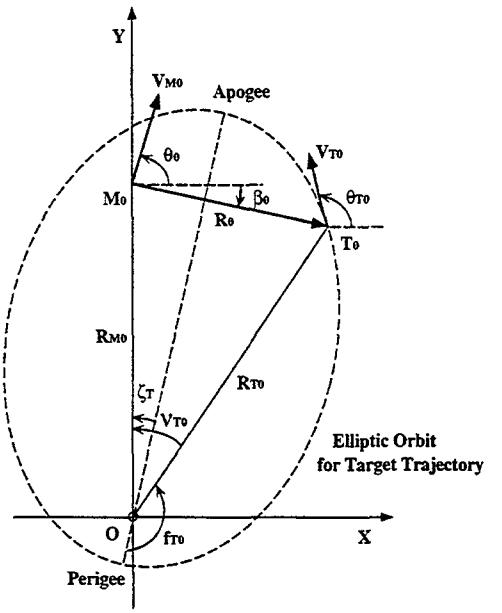

Fig. 7: Geometry for Elliptic Target Trajectory.

We now use the explicit solutions to study the interception of an incoming maneuvering long range ballistic missile. The geometry of the planar trajectory is shown in Fig. 7. The Cartesian coordinates system is set up such that O is the center of the Earth with OY along the direction to the initial position M_0 of the interceptor, which has the initial velocity $\mathbf{V}_{M0}$ with heading angle θ_0. At the initial time, the target is at the position $\mathbf{R}_0$ from M_0, with initial velocity $\mathbf{V}_{T0}$ with heading angle θ_{T0}. The ballistic trajectory is usually an arc of a highly elliptic orbit around its apogee. Let R_T be the distance to the target position from the center of the Earth. The polar equation of the elliptic orbit is

$$R_T = \frac{a_T(1 - e_T^2)}{1 + e_T \cos \mathrm{f}_T}. \qquad (33)$$

where a_T is semi-major axis, e_T is eccentricity of the trajectory, and f_T is the true anomaly.

The initial position of the target is conveniently defined by R_0 and β_0, and β_0 can be negative. Let R_{M0} be the initial radius of the interceptor. We use the normalized lengths

$$\rho_{M0} = \frac{R_{M0}}{R_0}, \quad \alpha_T = \frac{a_T}{R_0}. \qquad (34)$$

The motion of the target is completely specified by the data ρ_{M0}, β_0, α_T and e_T at the time $t_0 = 0$. Indeed, we now show that f_{T0}, the initial true anomaly from the perigee and ζ_T, the angle of the apogee from the y-axis and other elements can be computed in terms of the given data. From the law of cosines on the triangle OM_0T_0, we have the normalized radial distance of the initial target position from the center of the Earth

$$\rho_{T0} = \frac{R_{T0}}{R_0} = \sqrt{1 + \rho_{M0}^2 + 2\rho_{M0}\sin\beta_0}. \tag{35}$$

Next, using the law of sines for the same triangle

$$\frac{1}{\sin\nu_{T0}} = \frac{\rho_{T0}}{\sin(90^\circ + \beta_0)} = \frac{\rho_{T0}}{\cos\beta_0}. \tag{36}$$

We can solve for ν_{T0}, that is, the initial angle of the target position from the y-axis

$$\sin\nu_{T0} = \frac{\cos\beta_0}{\sqrt{1 + \rho_{M0}^2 + 2\rho_{M0}\sin\beta_0}}. \tag{37}$$

From Eq.(33) and Eq.(35), we have

$$1 + e_T\cos\mathrm{f}_{T0} = \frac{\alpha_T(1 - e_T^2)}{\sqrt{1 + \rho_{M0}^2 + 2\rho_{M0}\sin\beta_0}}. \tag{38}$$

Therefore, if ρ_{M0}, β_0, α_T and e_T are given as specified above, we can compute ρ_{T0} by Eq.(35), ν_{T0} by Eq.(37), and f_{T0} by Eq.(38). Then, as in Fig. 7, the angle ζ_T is simply calculated by

$$\zeta_T = (\mathrm{f}_{T0} + \nu_{T0}) - 180^\circ. \tag{39}$$

The initial speed of the target is evaluated by the energy integral and its heading is

$$\theta_{T0} = 180^\circ - (\nu_{T0} + \gamma_{T0}), \tag{40}$$

where γ_{T0} is the initial flight path angle with

$$\tan\gamma_{T0} = \frac{e_T\sin\mathrm{f}_{T0}}{1 + e_T\cos\mathrm{f}_{T0}}. \tag{41}$$

Equations of Motions

With respect to the normalized coordinate system M_0xy, we have

$$x_T = \frac{\alpha_T(1 - e_T^2)\sin(\mathrm{f}_T - \zeta_T)}{1 + e_T\cos\mathrm{f}_T}, \tag{42a}$$

$$y_T = -\frac{\alpha_T(1 - e_T^2)\cos(\mathrm{f}_T - \zeta_T)}{1 + e_T\cos\mathrm{f}_T}. \tag{42b}$$

The coordinates are functions of the true anomaly f_T, related to the eccentric anomaly E_T by

$$\tan\frac{E_T}{2} = \sqrt{\frac{1 - e_T}{1 + e_T}}\tan\frac{\mathrm{f}_T}{2}. \tag{43}$$

From Kepler's equation, if t is the time from f_{T0}, that is, from the corresponding E_{T0}, we have

$$\mathcal{M}_T = \sqrt{\frac{\mu}{a_T^3}}\ t = (E_T - E_{T0}) - e_T(\sin E_T - \sin E_{T0}), \tag{44}$$

where μ is the gravitational constant and $\mathcal{M}_T$ is the mean anomaly.

Equations (25), with the z-component omitted are used to obtain the coordinates x_M and y_M of the interceptor once the functions $r(\tilde{\tau})$ and $\beta(\tilde{\tau})$ are evaluated. This requires the selection of a pair of navigation constants k_1 and k_2 and the evaluation of A and u_0 as has been done in the preceding section. For the time transformation, we go from the true anomaly f_T to the mean anomaly M_T which is related to the time τ by [10]

$$\frac{\mathcal{M}_T}{\tau} = \frac{\sqrt{\mu/R_0}}{\alpha_T^{3/2}V_{T0}} = \frac{\sqrt{1 - e_T^2}}{\alpha_T\sqrt{1 + e_T^2 + 2e_T\cos\mathrm{f}_{T0}}}. \tag{45}$$

Now, from τ to $\tilde{\tau}$, with the conversion factor given in Eq.(30), and for the planar case where $\bar{V} = V$, we have

$$A = \frac{\tilde{\tau}}{\tau} = \sin(\theta_{T0} - \beta_0) - n_0\sin(\theta_0 - \beta_0), \tag{46}$$

where

$$n_0 = \frac{V_{M0}}{V_{T0}}, \tag{47}$$

is the initial speed ratio. Then, we have directly from $\mathcal{M}_T$ to $\tilde{\tau}$

$$\mathcal{M}_T = \frac{\sqrt{1 - e_T^2}\ \tilde{\tau}}{\alpha_T\ A\ \sqrt{1 + e_T^2 + 2e_T\cos\mathrm{f}_{T0}}}. \tag{48}$$

The initial closing speed, which has been given in Eq.(32), is now rewritten in terms of n_0 as

$$u_0 = \frac{\cos(\theta_{T0} - \beta_0) - n_0\cos(\theta_0 - \beta_0)}{\sin(\theta_{T0} - \beta_0) - n_0\sin(\theta_0 - \beta_0)}. \tag{49}$$

Therefore, in addition to the pair of navigation constants k_1 and k_2, the intercept trajectory depends on the initial engagement velocity of the interceptor represented here by n_0 and θ_0.

Let us now define the dimensionless speeds of target and interceptor. With respect to $\tilde{\tau}$, the rate of

change of the dimensionless linear range is $dr/d\tilde{\tau} = (1/\omega_{z0}R_0)(dR/dt)$. Hence the reference speed is $\omega_{z0}R_0$ and consequently we define

$$\tilde{v}_T(\tilde{\tau}) = \frac{V_T}{\omega_{z0}R_0}, \qquad \tilde{v}_M(\tilde{\tau}) = \frac{V_M}{\omega_{z0}R_0}. \tag{50}$$

From Fig. 4 we have the relative velocity along the line-of-sight and the direction orthogonal to it

$$r' = \tilde{v}_T\cos(\theta_T-\beta) - \tilde{v}_M\cos(\theta-\beta), \tag{51a}$$
$$r\beta' = \tilde{v}_T\sin(\theta_T-\beta) - \tilde{v}_M\sin(\theta-\beta). \tag{51b}$$

Hence, we have

$$\tilde{v}_M\cos(\theta-\beta) = \tilde{v}_T\cos(\theta_T-\beta) - r', \tag{52a}$$
$$\tilde{v}_M\sin(\theta-\beta) = \tilde{v}_T\sin(\theta_T-\beta) - r\beta'. \tag{52b}$$

Squaring and adding them, we have the general expression of the dimensionless speed of the interceptor

$$\tilde{v}_M^2 = \tilde{v}_T^2 + r'^2 + r^2\beta'^2 - 2\tilde{v}_T[r\beta'\sin(\theta_T-\beta) + r'\cos(\theta_T-\beta)]. \tag{53}$$

We define

$$u = \frac{r'}{r^{k_1-1}}. \tag{54}$$

By using this equation for r' and Eq.(8b) for $r\beta' = r^{k_1-1}$, we put the expression for $\tilde{v}_M^2$ in the form

$$\tilde{v}_M^2 = \tilde{v}_T^2 + r^{2(k_1-1)}(1+u^2) - 2\tilde{v}_T r^{k_1-1}[\sin(\theta_T-\beta) + u\cos(\theta_T-\beta)]. \tag{55}$$

In practice, it is more convenient to use V_{T0} as the unit speed, and we define

$$v_T = \frac{V_T}{V_{T0}}, \qquad v_M = \frac{V_M}{V_{T0}}, \tag{56}$$

with the conversion factor A from Eq.(46). Hence, by multiplying Eq.(56) by A^2, we have

$$v_M^2 = v_T^2 + r^{2(k_1-1)}A^2(1+u^2) - 2v_T r^{k_1-1}A\,[\sin(\theta_T-\beta) + u\cos(\theta_T-\beta)], \tag{57}$$

where v_T is evaluated according to [10]

$$v_T = \frac{\sqrt{1+e_T^2+2e_T\cos f_T}}{\sqrt{1+e_T^2+2e_T\cos f_{T0}}}. \tag{58}$$

As for the function u defined in Eq.(54), by taking the derivative of Eq.(10) with respect to $\tilde{\tau}$, we have

$$u = \frac{u_1 - u_2 C\exp[-K(\beta-\beta_0)]}{1 - C\exp[-K(\beta-\beta_0)}, \tag{59}$$

where

$$C = \frac{u_1-u_0}{u_2-u_0}. \tag{60}$$

Numerical Example

We consider the case of a ballistic missile with $\rho_{M0} = 1.9320$, $\beta_0 = -15°$, $\alpha_T = 1.232$ and $e_T = 0.754$. Then we can calculate

$$\rho_{T0} = \sqrt{1+\rho_{M0}^2 + 2\rho_{M0}\sin\beta_0} = 1.9320, \tag{61a}$$

$$\nu_{T0} = \arcsin\left(\frac{\cos\beta_0}{\rho_{T0}}\right) = 29.9978°, \tag{61b}$$

$$f_{T0} = \arccos\left\{\frac{1}{e_T}\left[\frac{\alpha_T(1-e_T^2)}{\rho_{T0}} - 1\right]\right\} = 164.0156°, \tag{61c}$$

$$\zeta_{T0} = (f_{T0}+\nu_{T0}) - 180° = 14.0134°, \tag{61d}$$

$$\gamma_{T0} = \arctan\left(\frac{e_T\sin f_{T0}}{1+e_T\cos f_{T0}}\right) = 37.0386°, \tag{61e}$$

$$\theta_{T0} = 180° - (\gamma_{T0}+\nu_{T0}) = 112.9636°. \tag{61f}$$

In Fig. 8, the target trajectory and intercept trajectories are plotted. We set $n_0 = 0.2$, $\theta_0 = 90°$, $k_1 = 3$ and $k_2 = 0$, 2, 3, 5. In all the cases, since the intercept condition is satisfied, the target is intercepted. But for the case of $k_2 = 0$, that is Cochran's law, theoretically the interceptor catches up with the target inside of the Earth (outside of the figure). But here, we have the freedom to choose the value of k_2 to adjust the time and position of interception. As can be seen from the figure, if we use larger values of k_2, we can intercept the target in an earlier stage. But in such a case, this requires a larger speed to fly the interceptor a longer distance in a shorter time as shown in Fig. 9. But here again, we have the freedom to choose k_2 to modify the velocity profile in order to keep the speed of the interceptor in an acceptable range.

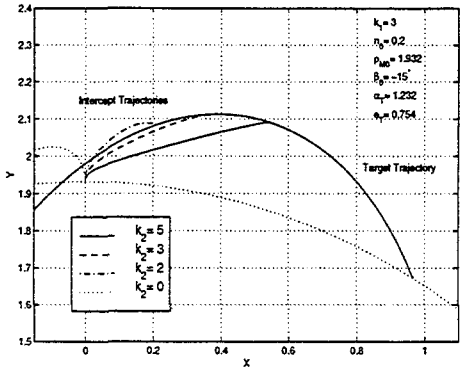

Fig. 8: Intercept Trajectories with various k_2.

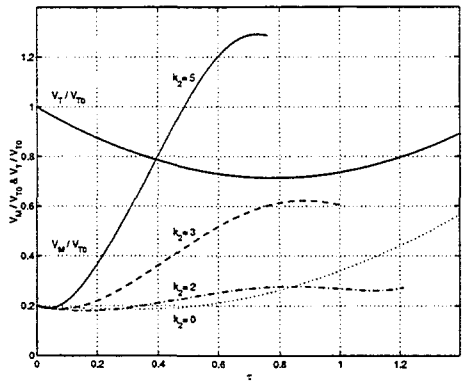

Fig. 9: Variation of Speed Ratio with various k_2.

Case of ICBM

Minimum Energy Trajectory

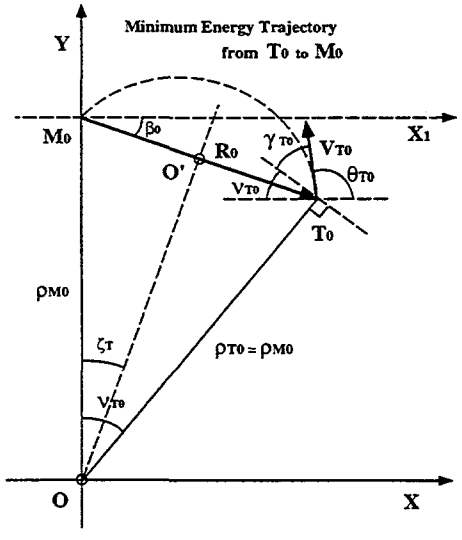

Fig. 10: Geometry of the Ideal Case for ICBM.

For the case of an intercontinental ballistic missile (ICBM) as a long-range ballistic-target in elliptic motion, its trajectory intersects the atmosphere. Since in these cases, to maximize the flight range with the available propulsion, the trajectory is usually near a minimum energy trajectory [3], the given elements, ρ_{M0}, β_0, α_T and e_T, are really not arbitrary.

As in Fig. 10, and for the sake of reducing the number of arbitrary parameters, we assume that $OT_0 = OM_0$ and hence we have

$$\rho_{T0} = \rho_{M0}. \tag{62}$$

From Eq.(35), we have

$$\sin\beta_0 = -\frac{1}{2\rho_{M0}}. \tag{63}$$

Therefore, using Eq.(36), we have

$$\sin\nu_{T0} = \frac{\cos\beta_0}{\rho_{M0}} = -2\sin\beta_0\cos\beta_0, \tag{64}$$

that is,

$$\nu_{T0} = -2\beta_0. \tag{65}$$

First, as a reference trajectory, we consider the minimum energy trajectory from T_0 to M_0. By a well known analysis Ref.[9], the second focus O' of the elliptic trajectory is on the segment M_0T_0. Furthermore, by symmetry, it is at the middle point. Hence, the major axis is

$$2\alpha_T = \rho_{M0} + \frac{1}{2}. \tag{66}$$

Then, again by symmetry

$$\zeta_T = -\beta_0, \tag{67}$$

and

$$\theta_{T0} = 180^\circ - (\gamma_{T0} + \nu_{T0}) = 180^\circ - (\gamma_{T0} - 2\beta_0). \tag{68}$$

It can be shown that [10]

$$\gamma_{T0} = 45^\circ - \frac{\nu_{T0}}{4} = 45^\circ + \frac{\beta_0}{2}. \tag{69}$$

Hence

$$\theta_{T0} = 135^\circ + \frac{3}{2}\beta_0. \tag{70}$$

Table 1: Data for Various ICBMs

D	ν_{T0}	ρ_{M0}
13,000 km	2.031250 rad (116.382 deg)	0.588367
10,000 km	1.562500 rad (89.525 deg)	0.710058
7,500 km	1.171875 rad (67.143 deg)	0.904191
5,000 km	0.781250 rad (44.762 deg)	1.313141
4,000 km	0.625000 rad (35.810 deg)	1.626341
3,000 km	0.468750 rad (26.857 deg)	2.152990
2,000 km	0.312500 rad (17.905 deg)	3.213058
1,000 km	0.156250 rad (8.952 deg)	6.406515
500 km	0.078125 rad (4.476 deg)	12.803256

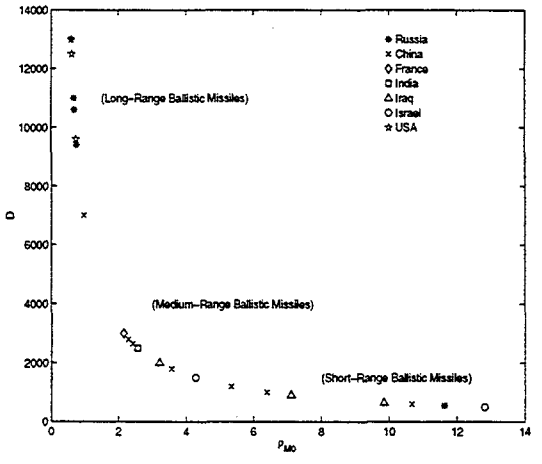

Fig. 11: Typical ICBMs (D>500km) from Various Countries.

This is the optimum angle for the initial velocity for a minimum energy trajectory passing through the point M_0.

The circumferential range is

$$D = R_{M0}\nu_{T0} = R_{M0}(-2\beta_0). \tag{71}$$

Taking a typical value, $R_{M0} = 6400km$, we can generate the table for the relationship between the circumferential range D, the initial separation angle ν_{T0} and the normalized initial distance of the interceptor from the center of the Earth ρ_{M0} as shown in Table 1. We have the plots of typical ranges for major ICBMs of Russia, China, France, India, Israel, Iraq and USA [4] in Fig. 11. As illustrative examples of ICBMs, the values of ρ_{M0} at 1.0, 3.0 and 10.0 are respectively typical values for long-range, medium-range and short-range ballistic trajectories. For the reference trajectory, since O' is the middle point of M_0T_0, the normalized conic parameter becomes

$$p_T = \frac{O'M_0}{R_0} = \alpha_T(1 - e_T^2) = \frac{1}{2}. \tag{72}$$

Then we can calculate the eccentricity by using α_T from Eq.(66)

$$e_T = \sqrt{\frac{\rho_{M0} - \frac{1}{2}}{\rho_{M0} + \frac{1}{2}}} = \frac{\cos\beta_0}{1 - \sin\beta_0}. \tag{73}$$

In conclusion, for $R_{M0} = R_{T0}$, and along a minimum energy trajectory passing through the point M_0, the elements β_0, α_T, e_T, ζ_T, ν_{T0},γ_{T0} and θ_{T0} are all expressible in terms of ρ_{M0}. In addition, from Eq.(39), (65) and (67) we have

$$f_{T0} = 180° + \beta_0. \tag{74}$$

From the energy integral, we calculate the reference speed on this minimum energy trajectory as

$$\frac{(V_{T0}^*)^2}{\mu/R_0} = \frac{2}{\rho_{T0}} - \frac{1}{\alpha_T} = \frac{2}{\rho_{T0}} - \frac{2}{\rho_{T0} + \frac{1}{2}} = \frac{1}{\rho_{T0}(\rho_{T0} + \frac{1}{2})}. \tag{75}$$

For the selected value of ρ_{M0} specifying the range of the ballistic trajectory, we generate typical near minimum energy trajectories as follows. By keeping fixed the direction of the initial velocity $\mathbf{V}_{T0}$, we decrease or increase its magnitude to have an undershoot or an overshoot trajectory. Geometrically, this corresponds to moving the second focus O' to O_1' at the distance $-\epsilon$ on the segment M_0T_0 or to O_2' by the distance ϵ as shown in Fig. 12. Therefore, with $\epsilon > 0$, we have the semi-major axis for the undershoot trajectory

$$\alpha_1 = \frac{1}{2}\left(\rho_{M0} + \frac{1}{2} - \epsilon\right). \tag{76}$$

On the contrary, for the overshoot trajectory, we use

$$\alpha_2 = \frac{1}{2}\left(\rho_{M0} + \frac{1}{2} + \epsilon\right). \tag{77}$$

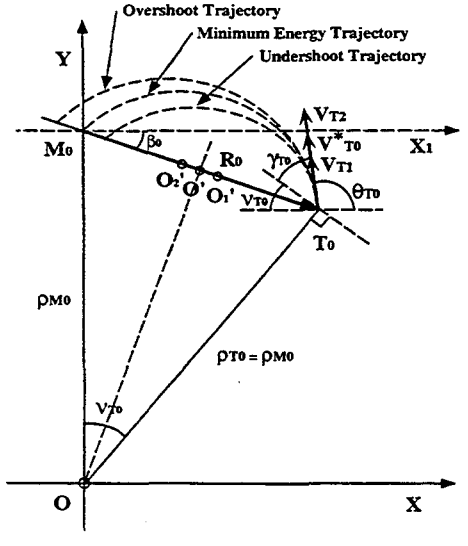

Fig. 12: Overshoot and Undershoot Trajectory of Elliptic Orbit.

For these trajectories, the values β_0, ν_{T0}, γ_{T0} and θ_{T0} remain the same, but because we have shifted the second focus to its new position on the segment M_0T_0, the values of the eccentricity e_T, the argument of the apogee ζ_T and the initial values of the

true anomaly f_{T0} change with ϵ. For the undershoot trajectory, we have

$$e_1 = \frac{OO_1'}{2\alpha_1} = \frac{\sqrt{\rho_{M0}^2 + \epsilon^2 - \frac{1}{4}}}{\rho_{M0} + \frac{1}{2} - \epsilon} > e_T. \qquad (78)$$

The value f_{T1} is computed from Eq.(38) with new values for α_1 and e_1 and ζ_{T1} is given by Eq.(39). We proceed the same way with the overshoot trajectory, starting with

$$e_2 = \frac{OO_2'}{2\alpha_2} = \frac{\sqrt{\rho_{M0}^2 + \epsilon^2 - \frac{1}{4}}}{\rho_{M0} + \frac{1}{2} + \epsilon} < e_T. \qquad (79)$$

As numerical examples, we take $\rho_{M0} = \rho_{T0} = 3.0$, as the case of a medium-range ($2,000km$ class) ballistic missile.

Through the discussion above, for given ρ_{M0}, we can calculate β_0, ν_{T0}, γ_{T0}, θ_{T0}, α_T, and the other elements of the minimum energy elliptic orbit for a target trajectory. With these values, we can draw the reference trajectory. Then, specifying ϵ as perturbation in the initial speed of the target, we can obtain the near-minimum energy trajectories, such as overshoot and undershoot trajectories.

For the minimum energy trajectory, we have $\beta_0 = -9.5941°$, $\nu_{T0} = 19.1882°$, $\zeta_{T0} = 9.5941°$, $\alpha_T = 1.7500$, $e_T = 0.8452$, $\gamma_{T0} = 40.2030°$, $f_{T0} = 170.4060°$ and $\theta_{T0} = 120.6089°$.

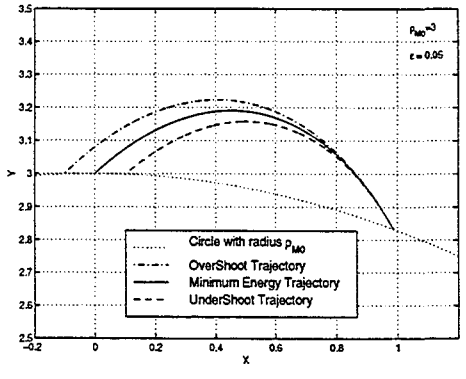

Fig. 13: Overshoot, Minimum Energy, and Undershoot Trajectories of Target with $\rho_{M0} = 3$ for Medium-Range Ballistic Missile.

For the two perturbed trajectories, we keep γ_{T0}, and hence also θ_{T0} the same, and take $\epsilon = 0.05$ to change the major axis. Then, for the undershoot trajectory, we have $\alpha_1 = 1.725$, $e_1 = 0.8575$, $f_{T1} = 171.3743°$, $\zeta_{T1} = 10.5625°$. For the overshoot trajectory, the computed data are $\alpha_2 = 1.7750$, $e_2 = 0.8334$, $f_{T2} = 169.4375°$, $\zeta_{T2} = 8.6257°$. The reference trajectory and the two perturbed trajectories are plotted in Fig. 13.

By following the sensitivity analysis discussed in Ref.[10], it can be shown that, to the order of ϵ, the change in the angular range is

$$\Delta\nu_T = \frac{4\epsilon}{\sqrt{4\rho_{M0}^2 - 1}}. \qquad (80)$$

Head-on Interception

Head-on interception is one of the good tactics to increase the accuracy of interception. Idan et al. [5] studied the head-on interception of a ballistic target as an optimal control problem with the constraint on the final approach angle. Since we have the complete analytical solution of our guidance law, we can easily do a parametric study to obtain head-on interception.

In order to intercept a target in head-on position, the head-on condition

$$\beta_f = \theta_f = \theta_{Tf} - \pi, \qquad (81)$$

is required. But if the condition of interception $u_0 < u_2$ (12) is already satisfied, the head-on condition is simply

$$\beta_f = \theta_{Tf} - \pi. \qquad (82)$$

Let us note that, here, we have θ_0 and n_0 to be selected as the engagement parameters. When the initial position of the target, such as β_0 and θ_{T0}, are given and either k_1 or k_2 is already set - for example we take k_1 - then for each pair of (n_0, θ_0) defining the initial velocity of the interceptor, we can adjust k_2 to satisfy the reduced head-on condition (82).

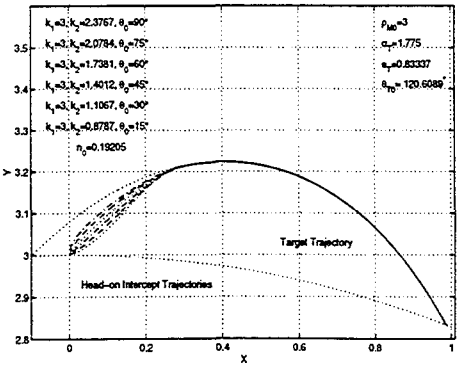

Fig. 14: Various Trajectories of Head-on Interception.

Example Let us take $\rho_{M0} = 3$ and $\epsilon = 0.05$ as an overshoot ballistic target trajectory with $\alpha_T =$

1.775, $e_T = 0.83337$, and an interceptor such that the initial speed $n_0 = 0.19205$, and one of the navigation constants k_1 set to be 3.

Now our choice is the initial heading angle θ_0 of the interceptor. We use $\theta_0 = 15°, 30°, 45°, 60°, 75°, 90°$ for possible engagement. Once we take one value of θ_0, another navigation constant k_2 is determined in order to satisfy the head-on condition (82). In Fig. 14, six head-on intercept trajectories are shown for the six values of θ_0 selected.

Delayed Launch

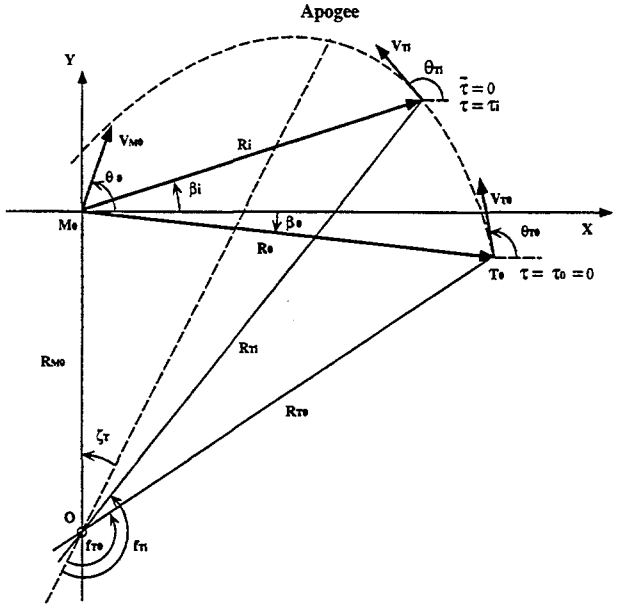

Fig. 15: Hypothetical Elliptic Trajectory of Target.

Until now, we set the target initial position T_0 where $\rho_{T0} = \rho_{M0}$. Usually, however, when the interceptor starts its homing flight at M_0, the target may be already on its way to impact. For such a case, we use the formulation of delayed launch. We first consider the hypothetical elliptic trajectory of target, starting at $\mathrm{f}_T = \mathrm{f}_{T0}$ as shown in Fig. 15. Since the true anomaly and the flight time are related, we use the true anomaly in the formulation instead of time. Let us assume that the interceptor is launched when the target is at $\mathrm{f}_T = \mathrm{f}_{Ti}$, that is, $\tau = \tau_i$. The target position at that time is such that

$$x_{Ti} = \frac{\alpha_T(1-e_T^2)\sin(\mathrm{f}_{Ti}-\zeta_T)}{1+e_T\cos\mathrm{f}_{Ti}}, \quad (83a)$$

$$y_{Ti} = -\frac{\alpha_T(1-e_T^2)\cos(\mathrm{f}_{Ti}-\zeta_T)}{1+e_T\cos\mathrm{f}_{Ti}}. \quad (83b)$$

and, its distance from the center of the Earth is

$$\rho_{Ti} = \frac{\alpha_T(1-e_T^2)}{1+e_T\cos\mathrm{f}_{Ti}}. \quad (84)$$

Using Eq.(83), we can calculate r_i and β_i as follows

$$r_i = \sqrt{x_{Ti}^2 + (y_{Ti}-\rho_{M0})^2}, \quad (85)$$

$$\tan\beta_i = \frac{y_{Ti}-\rho_{M0}}{x_{Ti}}. \quad (86)$$

Recalling Eq.(58)

$$\mathrm{v}_{Ti} = \frac{V_{Ti}}{V_{T0}} = \frac{\sqrt{1+e_T^2+2e_T\cos\mathrm{f}_{Ti}}}{\sqrt{1+e_T^2+2e_T\cos\mathrm{f}_{T0}}}, \quad (87)$$

and keeping the same initial speed of the interceptor V_{M0} for every engagement, we have the initial speed ratio for each delayed launch as

$$n_i = \frac{V_{M0}}{V_{Ti}} = \frac{V_{M0}}{V_{T0}}\frac{V_{T0}}{V_{Ti}} = \frac{n_0}{\mathrm{v}_{Ti}} = n_0\frac{\sqrt{1+e_T^2+2e_T\cos\mathrm{f}_{T0}}}{\sqrt{1+e_T^2+2e_T\cos\mathrm{f}_{Ti}}}. \quad (88)$$

Next modifying Eq.(41), we have the target flight path angle between the target velocity vector and the local horizontal when $\mathrm{f}_T = \mathrm{f}_{Ti}$ as

$$\tan\gamma_{Ti} = \frac{e_T\sin\mathrm{f}_{Ti}}{1+e_T\cos\mathrm{f}_{Ti}}, \quad (89)$$

and using Eqs.(39) and (40), we obtain the target heading angle at that time

$$\theta_{Ti} = \mathrm{f}_{Ti} - \zeta_T - \gamma_{Ti}. \quad (90)$$

With β_i in Eq.(86), θ_{Ti} in Eq.(90) and $\theta_i = \theta_0$, we now calculate the initial closing speed u_i at the delayed launch time τ_i from Eq.(49) as

$$u_i = \frac{\cos(\theta_{Ti}-\beta_i) - n_i\cos(\theta_i-\beta_i)}{\sin(\theta_{Ti}-\beta_i) - n_i\sin(\theta_i-\beta_i)}. \quad (91)$$

Also we have from Eq.(46)

$$A_i = \frac{\mathrm{v}_{Ti}}{r_i}\left[\sin(\theta_{Ti}-\beta_i) - n_i\sin(\theta_i-\beta_i)\right], \quad (92)$$

for the time scale conversion from $\bar{\tau}$ for the delayed interception to τ for the first interception launched at $\mathrm{f}_T = \mathrm{f}_{T0}$.

Now let us consider the procedure of the delayed launch. For the analytical solution of relative motion, we must solve the differential equations (8a) and (8b) of the guidance system in each time scale of $\bar{\tau}$ for each

engagement. For the calculation of the i-th interception, we reset the initial conditions to

$$\tilde{r}(\tilde{\tau}=0) = 1, \quad (93a)$$
$$\beta(\tilde{\tau}=0) = \beta_i, \quad (93b)$$
$$\tilde{r}'(\tilde{\tau}=0) = u_i. \quad (93c)$$

Once we have the solution of the relative motion between target and interceptor, that is, $\tilde{r}(\tilde{\tau})$ and $\beta(\tilde{\tau})$, using Eqs.(5), we calculate the position of interceptor from the target position in the normalized coordinate. After the time conversion to τ with A_i from the equation

$$\tau = \frac{\tilde{\tau}}{A_i} + \tau_i, \quad (94)$$

for each engagement, and the necessary scale conversion with

$$R = R_0\, r_i\, \tilde{r}, \quad (95)$$

we obtain the original-scale trajectory of the interceptor.

Example As an example, we use again the overshoot target trajectory with $\rho_{M0} = 3$ and $\epsilon = 0.05$. We then launch an interceptor without delay at $\tau = 0$, when the target is at $f_{T0} = 169.4375°$, and intercept it at P_0 using $n_0 = 0.19205$, $\theta_0 = 45°$ and $k_1 = 3$, $k_2 = 2$. The first, second, third delayed launches at $\tau_1 = 0.0980$, $\tau_2 = 0.2030$, $\tau_3 = 0.3122$ are when the targets are at the true anomalies $f_{T1} = 172.6356°$, $f_{T2} = 175.8336°$, $f_{T3} = 179.0316°$, respectively. The resulting intercept trajectories are depicted in Fig. 16. The variations of the corresponding speed of the target and the interceptor are plotted in Fig. 17. Although the non-delayed launch leads to early interception, the duration of the interception is long. In the case 3, the intercept time is short, but it requires larger velocity than that of the case 2. If we choose case 2, the velocity change of the interceptor is smallest.

So the benefit of the delayed launch is not only to increase the kill probability but also to be able to modify the velocity profile of the interceptor and to keep the velocity in an acceptable range. Of course, the concept and the formulation of the delayed launch is applied to the so-called "shoot-look-shoot" strategy [6] to increase the chances of successful engagement to defend vital areas from the threat of the incoming ballistic targets.

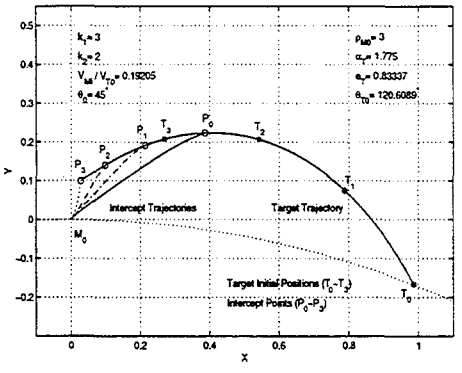

Fig. 16: Intercept Trajectories of Delayed Launch.

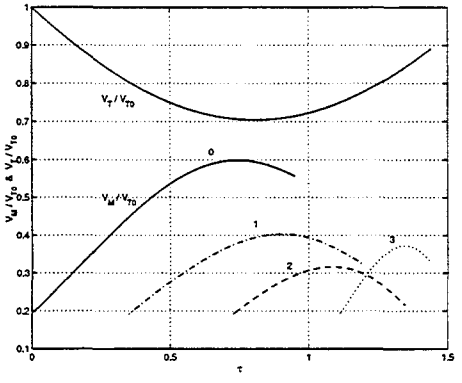

Fig. 17: Variation of Speed of Delayed Launched Interceptors.

Realization of the Guidance Law

The Required Thrust

We now consider the realization of this guidance law for the case of interception of a target on an elliptic trajectory in a central inverse square force field as in Fig. 18.

By taking the second derivatives of Eqs.(5a) and (5b), we have the equations for the acceleration of the interceptor

$$\ddot{X}_M = \ddot{X}_T - \frac{d^2}{dt^2}(R\cos\beta), \quad (96a)$$
$$\ddot{Y}_M = \ddot{Y}_T - \frac{d^2}{dt^2}(R\sin\beta). \quad (96b)$$

Since the target is under the central inverse square force field, we have the equations

$$\ddot{X}_T = -\mu\frac{X_T}{R_T^3}, \quad (97a)$$
$$\ddot{Y}_T = -\mu\frac{Y_T}{R_T^3}. \quad (97b)$$

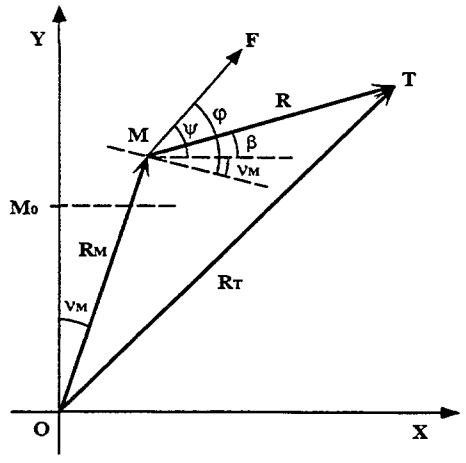

Fig. 18: Geometry for Powered Flight.

On the other hand, for the interceptor, we have

$$\ddot{X}_M = -\mu\frac{X_M}{R_M^3} + F\cos\psi, \tag{98a}$$

$$\ddot{Y}_M = -\mu\frac{Y_M}{R_M^3} + F\sin\psi, \tag{98b}$$

where F is the thrust acceleration and ψ is thrust angle for the powered flight.

By substituting Eqs.(97) and Eqs.(98) into Eqs.(96), and using the derivative in $\bar{\tau} = \omega_{z0}\, t$, we have

$$F\cos\psi = \frac{\mu}{R_0^2}\frac{x_M}{\rho_M^3} - \frac{\mu}{R_0^2}\frac{x_T}{\rho_T^3} - \omega_{z0}^2 R_0\,(r\cos\beta)'', \tag{99a}$$

$$F\sin\psi = \frac{\mu}{R_0^2}\frac{y_M}{\rho_M^3} - \frac{\mu}{R_0^2}\frac{y_T}{\rho_T^3} - \omega_{z0}^2 R_0\,(r\sin\beta)''. \tag{99b}$$

We define the normalized thrust acceleration f and a new parameter B with Eqs.(46) and (75)

$$f = \frac{F}{\omega_{z0}^2 R_0}, \tag{100}$$

$$B = \frac{\mu}{\omega_{z0}^2 R_0^3} = \frac{\alpha_T\,\rho_{T0}}{(2\alpha_T - \rho_{T0})\,A^2}. \tag{101}$$

Then, we have the normalized form of Eqs.(99), that is the x- and y-components of the dimensionless thrust acceleration

$$f_x \equiv f\cos\psi = B\left(\frac{x_M}{\rho_M^3} - \frac{x_T}{\rho_T^3}\right) - (r\cos\beta)'', \tag{102a}$$

$$f_y \equiv f\sin\psi = B\left(\frac{y_M}{\rho_M^3} - \frac{y_T}{\rho_T^3}\right) - (r\sin\beta)''. \tag{102b}$$

The dimensionless thrust acceleration and the thrust angle for the powered flight can then be computed as

$$f^2 = f_x^2 + f_y^2, \tag{103}$$

$$\tan\psi = \frac{f_y}{f_x}. \tag{104}$$

The thrust angle from the local horizontal can also be obtained as

$$\varphi = \psi + \nu_M, \tag{105}$$

where ν_M is the angle of the position of interceptor from y-axis as in Fig. 18 with

$$\tan\nu_M = \frac{X_M}{Y_M}. \tag{106}$$

It is convenient to express the thrust magnitude in the form of the thrust-to-weight ratio F/g

$$\frac{F}{g} = \frac{f}{B}\,\rho_M^2. \tag{107}$$

Also, it can be shown that the thrust acceleration tends to zero at the final time if $k_1 > 2$.

Example As an example, we use the overshoot target trajectory, which is the solid line in Fig. 19, in the case of $\rho_{M0} = 3$ with $\epsilon = 0.05$ and hence $\beta_0 = -9.5941°$, $\alpha_T = 1.7750$ and $e_T = 0.8334$. Setting $k_1 = 4$, $k_2 = 3$, $\theta_0 = 60°$, $n_0 = 0.3841$, we first have the analytical intercept trajectory obtained by the analytical solution of the guidance law, as the dash-dot line in Fig. 19. Next, by using the thrust law above, we calculate the thrust angle ψ and the thrust-to-weight ratio F/g for the powered flight as in Figs. 20 and 21, respectively. Then applying that thrust law, we integrate numerically the equations of motion of the interceptor to obtain the powered flight intercept trajectory in Fig. 19. As can be seen in this figure, both analytical and powered flight trajectories show perfect agreement.

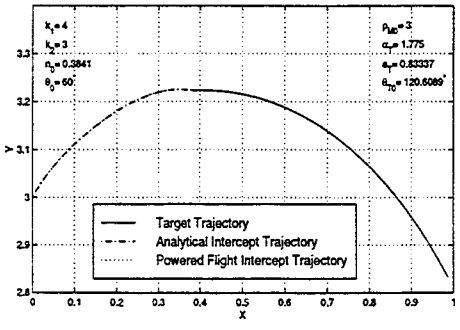

Fig. 19: Analytical Intercept Trajectory and Powered Flight Intercept Trajectory.

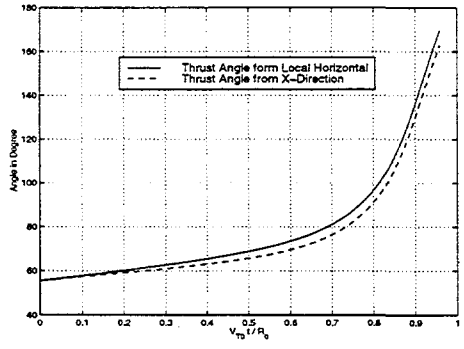

Fig. 20: Variation of Thrust Angle.

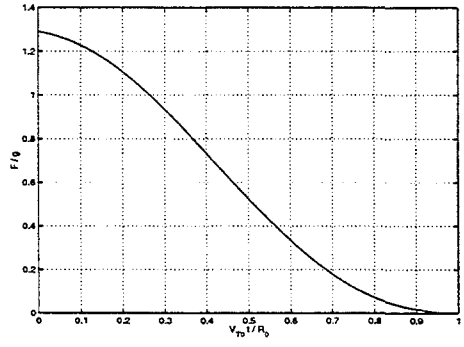

Fig. 21: Variation of Thrust-to-Weight Ratio.

Optimal Interception

By specifying the final time τ_f, we specify the intercept position $(x_f,\ y_f)$. We then can use Lambert's theorem to calculate the initial condition n_{0L} and θ_{0L} for the interceptor to be on a collision course on free flight with the target. It can be said that, if the guided intercept trajectory coincides with the Lambert trajectory, the interceptor does not need any thrust acceleration during its flight, apart from the gravitational acceleration. To follow the Lambert trajectory, we use this initial elliptic targeting condition for the powered flight interceptor, which has two navigation constants k_1 and k_2 for homing towards the target. Since theoretically, without thrusting correction, the Lambert condition leads to interception, it is possible to select a pair of parameters $(k_1,\ k_2)$ for minimum fuel consumption with the guidance law enforced.

For the powered flight, we have the equation for the mass flow rate [7, 8]

$$\frac{dm}{dt} = -\frac{c}{g}T. \tag{108}$$

where c is the specific fuel consumption, m is the mass, and T is the thrust of the interceptor. Since we have the relation $T = m\,F$, using $\tau = (V_{T0}/R_0)\,t$, we have

$$-\frac{dm}{m} = \left(\frac{cR_0}{V_{T0}}\right)\left(\frac{F}{g}\right)d\tau. \tag{109}$$

Hence, we define the performance index for the minimum-fuel powered flight as

$$J = \left(\frac{V_{T0}}{cR_0}\right)\log\frac{m_0}{m_f} = \int_0^{\tau_f}\left(\frac{F}{g}\right)d\tau, \tag{110}$$

with the constraint such as

$$\Delta\tau = \tau_f(k_1, k_2), \tag{111}$$

where $\Delta\tau$ is the specified time of interception. Our purpose is to minimize this performance index J with respect to k_1 and k_2.

The procedure to achieve this optimal interception is as follows. First, we are given the specified intercept time τ_f or equivalently the specified intercept point $(x_f,\ y_f)$. Next, from that given condition, we solve the Lambert problem to obtain the initial elliptic targeting condition n_{0L} and θ_{0L}. Then we have n_{0L}, θ_{0L} and θ_{T0}, β_0 in order to calculate A and u_0

$$A = \sin(\theta_{T0} - \beta_0) - n_{0L}\sin(\theta_{0L} - \beta_0), \tag{112a}$$

$$u_0 = \frac{\cos(\theta_{T0} - \beta_0) - n_{0L}\cos(\theta_{0L} - \beta_0)}{\sin(\theta_{T0} - \beta_0) - n_{0L}\sin(\theta_{0L} - \beta_0)}. \tag{112b}$$

Once u_0 is obtained, τ_f becomes function of k_1 and k_2 only in Eq.(18), and there exist pairs of k_1 and k_2 to satisfy the final time constraint τ_f. Then, we set some values of k_2, and find the corresponding values of k_1 which satisfy the specified intercept time τ_f. Finally, for each pair of k_1 and k_2, we calculate the thrust accelerations and integrate them to find out the optimal pair of k_1 and k_2 which minimizes the performance index J, that is the total fuel consumption.

Example Taking $\rho_{M0} = 3$ and $\epsilon = 0$ for a minimum energy ballistic target trajectory, we specify the normalized intercept time as $\tau_f = 0.96129$, and calculate the intercept position in dimensionless coordinate as $(x_f,\ y_f) = (0.3691,\ 3.1840)$. Then upon solving the Lambert problem, we have the initial elliptic targeting condition $n_{0L} = 0.80989$, and $\theta_{0L} = 60.0973°$. Now to compensate for possible error in targeting, we use these conditions for the powered flight with a pair of navigation constants k_1 and k_2 to make the interceptor home to the target.

For each k_2 used as a parameter, the corresponding k_1 is determined to satisfy the constraint on τ_f at

$r_f = 0$. For this trajectory, the thrust-to-weight ratio is generated and the integral (110) is evaluated for the performance index J which is plotted in Fig. 22 in terms of k_2. Its minimum $J_{min} = 0.0091228$ occurs at $k_2 = 90.99$ with the corresponding $k_1 = 3.307$.

It is noted that, by our normalization the analysis is independent of the mass of the planet of attraction and of the characteristics of the fuel used. To have a physically realistic instance, we take the Earth with $\mu = 3.986 \times 10^5 km^3/s^2$, and a typical value $R_{M0} = 6378 + 22 = 6400km$. Then with $\rho_{M0} = 3$, we have $R_0 = 2133.33km$, $V_{T0} = 4.218km/s$. If the fuel used is such that $1/c = 400sec$, with J_{min} computed above, we have the fuel ratio $\Delta m_{fuel}/m_0 = 0.011$.

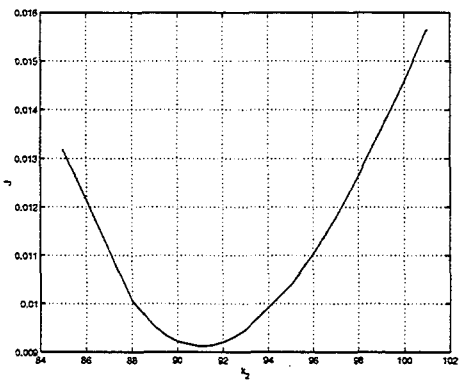

Fig. 22: Performance Index J with Various k_2.

Conclusions

A new guidance law, with explicit solutions, is applied for interception of a long range missile. In the absence of atmosphere, the ballistic flight path of the target is generally an arc of a highly eccentric ellipse. The minimum-fuel ballistic intercept trajectory can be easily obtained via Lawden primer vector theory. But if the target trajectory is perturbed, or if the error in tracking leads to a miss distance in interception in the pure ballistic mode, the guidance law, if activated, will lead the interceptor in homing to the target. It is shown that by a rotation of coordinate system, the problem of three-dimensional interception is reduced to a planar problem. The general case of planar interception of a long range ballistic missile is then studied. The equations of motion of the interceptor in its homing flight path, the variation of its speed and the thrust law for the guidance are given in explicit forms. Examples of interception at a specified time, head-on interception and minimum-fuel interception are presented.

References

1. Abramowitz, M. and Stegun, I. A., *Handbook of Mathematical Functions*, National Bureau of Standard, Washington D.C., 1964.

2. Cochran Jr., J. E., No, T. S., and Thaxton, D. G., "Analytical Solutions to a Guidance Problem", *Journal of Guidance, Control and Dynamics*, Vol.14, No.1, Jan.-Feb. 1991, pp.117-122.

3. Garwin, R. L., and Bethe, H. A., "Anti-Ballistic-Missile Systems", *Scientific American*, Vol. 218, No 3, 1968, pp.21-31.

4. Gunston, B., *The Illustrated Encyclopedia of the World's Rockets and Missiles*, Crescent Books, New York, 1979.

5. Idan, M., Golan, O. M., and Guelman, M., "Optimal Planar Interception with Terminal Constraints," *Journal of Guidance, Control, and Dynamics*, Vol.18, No.6, 1995, pp.1273-1279.

6. Mosher, D. E., "The Grand Plans", *IEEE Spectrum*, Vol.34, No.9, 1997, pp.28-39.

7. Vinh, N. X., *Flight Mechanics of High-Performance Aircraft*, Cambridge University Press, Cambridge, Great Britain, 1993.

8. Vinh, N. X., *Optimal Trajectories in Atmospheric Flight*, Elservier Scientific Publication Co., Amsterdam, The Netherlands, 1981.

9. Vinh, N. X., and Arora, K., L., "Maximum Range of Ballistic Missile," *SIAM Review*, Oct., 1965, pp.544-550.

10. Vinh, N. X., Busemann, A., and Culp, R. D., *Hypersonic and Planetary Entry Flight Mechanics*, The University of Michigan Press, Ann Arbor, MI, 1980.

11. Vinh, N. X., Kabamba, P. T., and Takehira, T., "Analytical Solution to a Three-Dimensional Interception of a Maneuvering Target", *AAS Paper No.98-132*, AAS/AIAA Space Flight Mechanics Meeting, Montery, CA., Feb.9-11, 1998.

12. Vinh, N. X., Lu, P., Howe, R. M. and Gilbert, E. G., "Optimal Interception with Time Constraint", *Journal of Optimization Theory and Applications*, Vol.66, No.3, Sep. 1990, pp.361-390.